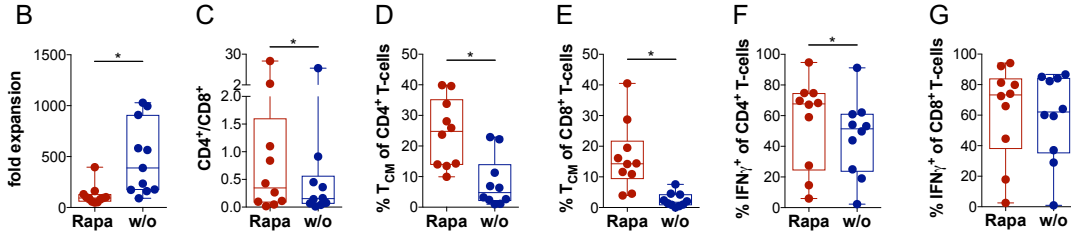
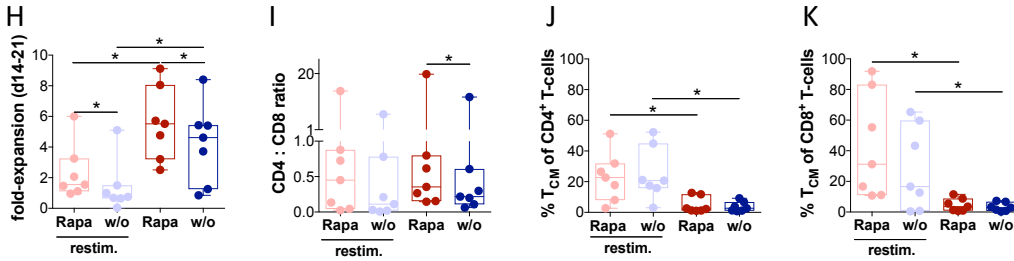


d14: Enrichment of CD4⁺ T-cells and T_{CM} at d14



d21: Recovered expansion rates at d21, antigen encounter decreases expansion rates, but promotes less differentiated cells



d49: Rapamycin preserves superior capacity for IFN γ production

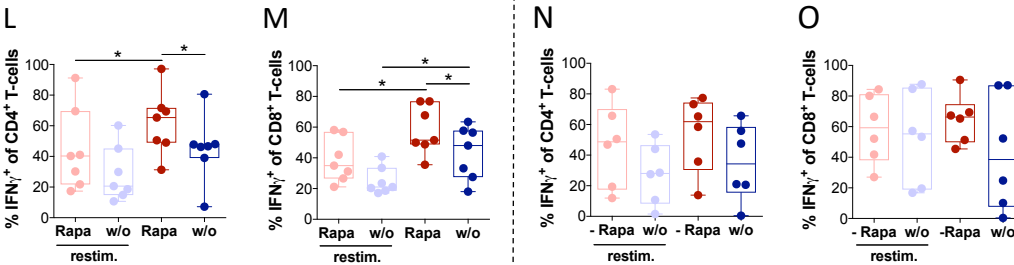


Figure S1: Effects of Rapamycin on IL-2/IL-7-expanded T-cell products: Expansion, phenotype and function

A: Schematic overview of experiments: T-cell products (TCPs) were generated from PBMCs isolated from venous blood of healthy donors (HDs) by magnetically activated cell isolation sorting (MACS) of T-cells producing IFN γ in response to stimulation with CMV_{IE-1/pp65} peptide pools and expanded in the presence of IL-2/IL-7 without (w/o; blue) or with addition of 20 nM of Rapamycin (Rapa; red). **B:** Expansion rates of IL-2/7-expanded Rapa-treated (Rapa-)TCPs (red) and untreated TCPs (blue) of n=10 healthy donors (HDs) calculated from yield at d14 divided by the number of seeded cells at d0. We gated flow cytometric data on lymphocytes → singlets → living CD3⁺ T-cells. **C:** CD4/CD8 ratios in Rapa- (red) and untreated TCPs (blue) of n=10 HDs calculated from flow cytometry data as presented in Fig. 1C. **D-E:** Proportions of CD4⁺ (**D**) and CD8⁺ T_{CM} (**E**) among Rapa- (red) and untreated TCPs (blue) of n=10 HDs determined from flow cytometric data as shown in Fig. 1E at d14. **F-G:** To detect CMV-specific cytokine producers, TCPs were stimulated with CMV_{IE-1/pp65} peptide-loaded autologous LCLs at a ratio of 1:10 for 6 h and BFA was added after 1 h. Proportions of CMV-specific IFN γ -producers among CD4⁺ (**F**) and CD8⁺ T-cells (**G**) in Rapa- (red) and untreated TCPs (blue) of n=10 HDs determined from flow cytometric data as shown in Fig. 1G at d14. **H-O:** For restimulation on d14 of culture, thawed CD3⁺ autologous PBMCs were loaded with CMV_{IE-1/pp65} peptide pools and added at 1:5 ratio to T-cells. **H:** Expansion rates of IL-2/7-expanded restimulated (pastel colors) or non-restimulated (dark colors) Rapa- (red) and untreated TCPs (blue) of n=7 HDs calculated from yield at d21 divided by the number of cells at d14. **I:** CD4/CD8 ratios in Rapa- (red) and untreated TCPs (blue) of n=7 HDs calculated from flow cytometric data as presented in Fig. 1C at d21. **J-K:** Proportions of CD4⁺ (**J**) and CD8⁺ T_{CM} (**K**) among Rapa- (red) and untreated TCPs (blue) of n = 7 HDs determined from flow cytometric data as shown in Fig. 1E at d21. **L-M:** To detect CMV-specific cytokine producers, TCPs were stimulated with CMV_{IE-1/pp65} peptide-loaded autologous LCLs for 6 h and BFA was added after 1 h. Proportions of CMV-specific IFN γ -producers among CD4⁺ (**L**) and CD8⁺ T-cells (**M**) in Rapa- (red) and untreated TCPs (blue) of n=7 HDs determined from flow cytometric data as shown in Fig. 1G at d21. **N-O:** To mimic the situation after infusion, Rapa was withdrawn and TCPs were cultivated long-term until d49. Proportions of CMV-specific IFN γ -producers among CD4⁺ (**N**) and CD8⁺ T-cells (**O**) in TCPs withdrawn from Rapa (red) and untreated TCPs (blue) of n=6 HDs determined from flow cytometric data as shown in Fig. 1G at d49. For all graphs normal distribution of data points was tested with Kolmogorov-Smirnov test and paired t test was used to determine significance in normally distributed samples or Wilcoxon's matched-pairs signed rank test in not normally distributed samples, respectively. P-values below 0.05 are indicated by * and defined to be significant.

Table S1: Differentially expressed genes. Log2-fold describes log2-fold expression of the respective gene in untreated vs. Rap2-TCPs.

	Ensemble ID	Gene	Function in T-cells	baseMean	log2Fold		Ensemble ID	Gene	Function in T-cells	baseMean	log2Fold	
LONG-LIVED MEMORY	PROMOTING											
	ENSG00000164530	PI16	unique subset of memory T helper $\alpha\alpha$ cells with hyperproliferative and proinflammatory properties (1)	135.857891	-4.52067	ENSG00000196507	TCEAL3	transcription elongation factor	98.9871397	-2.19082		
	ENSG00000163813	CCRA	innate CD8 T cell memory subset (2)	228.819399	-3.97254	ENSG00000175155	YPEL2	part of the mitotic apparatus required for cell division (83)	1404.32006	-1.19115		
	ENSG00000128353	CCR7	Tau marker (3)	2184.22723	-3.76723	ENSG00000048886	CH3L2	activation of ERK1/2 phosphorylation by CH3L2 inhibits cell mitogenesis and proliferation (84)	183.237131	1.18076		
	ENSG00000056736	IL17RB	highest expression in CD4+ T cells expressing prostaglandin receptor D2 (T1u) (4)	3717.7812	-1.98748	ENSG00000102302	NME4	involved in Pyrimidine Metabolism and Metabolism	325.68844	-1.87288		
	ENSG00000204252	HLA-DQA	non-classical MHC class II (peptide loading), higher expression in CD8 CD28+ T-cells from young than from old subjects (5)	1363.3723	-2.28921	ENSG00000174136	RGMB	involved in T cell activation and supports T-cell expansion (67)	181.82579	-2.82547		
	ENSG00000073331	ALPK1	target of Tet-1 (6) downstream of Akt (arresting memory CD8+ T-cell differentiation (7))	404.02766	-1.89246	TNFRSF19	cell cycle regulated NADPH-dependent dicarboxylate reductase enzyme (85)	52.286621	-2.60785			
	ENSG00000135318	TERE	CD73 catalyses the conversion of extracellular nucleotides to membrane-permeable nucleosides, CD73+ mouse memory CD4+ T-cells make IL-2, but less IFN γ than CD73- (8)	278.662059	-2.20378	DHR22	ligand for UDP-glucose, activation inhibits murine T cell proliferation (86)	68.738987	-2.18412			
	ENSG00000164362	NKX2	Telomerase reverse transcriptase, overexpression extends proliferative potential of human T-cells (9)	27.7024907	-3.43006	ENSG00000164362	TERT	Telomerase Reverse Transcriptase, overexpression extends proliferative potential of human T-cells (9)	27.7024907	-3.43006		
	ENSG00000116016	ELP1	allows Tau expansion in Rapamycin (10), antipoptotic/upregulated in Tau vs. Tau (11)	7644.0849	-1.735721	ENSG0000011860	CSMR1	enhances naive CD4+ T-cell activation, survival and proliferation via PI3K/Akt (50)	200.01984	-2.11075		
	ENSG00000168885	ILTR	accumulates upon early TCR signaling and hypoxia, accumulation increases glycolysis/G2M, expression diminished upon administration of IL-2, increased upon administration of IL-4, sustained effector function of CD8 CTLs (12)	3957.70915	-1.55463							
	ENSG00000132170	PPARG	identifies the effector CD8 memory T-cell precursors that can persist and confer protective immunity (13)	11962.7635	-2.044891							
	ENSG00000072110	ACTN1	required for long-term persistence of CD8+ T-cells in the skin, upregulated on Tau (14)	391.15506	-2.14384							
	ENSG00000143674	MAP3K21	downregulated in effector/exhausted murine T-cells compared to memory T-cells (15)	1155.07765	-1.455754							
	ENSG00000140343	IGF1R	bivalent methylation in CD8+ Tc and Tau allows rapid switch from a resting to activated state, transcription increased upon activation (16)	193.130633	-1.70155							
	ENSG00000159896	PLCL1	increased in autoimmunity, increased upon TCR stimulation, ligand binding enhances proliferation and survival of CD45RO+ T-cells (17)	797.424827	-1.791784							
	ENSG00000140423	IGFBP3	CD25 methylation decreased in memory vs. naive CD4+ upregulated upon activation with CD3/CD28 for 48 h (18)	2484.05367	-2.708713							
	ENSG00000162490	DRAXN	antagonist of Wnt signaling (20)	221.61933	1.84185							
	ENSG00000148053	NTRK2	downregulated on CD4+ CD62L+ T-cells compared to CD62L- (21)	608.962631	-2.751809							
	ENSG00000149295	DRD2	dopamine receptor, drives Tau differentiation via T-bet and IFN γ production, decreases CD25 and CD69, advances T-cell differentiation, helps NFkB activation (22)	30.4424689	-3.125411							
EFFECTOR FUNCTION	ENSG00000173334	TRIB1	in transplant patients marker of ongoing immune activation and an antibody response (23), 40 higher expression in T_{H1} than T_{H2} , but 47 of culture higher expression in T_{H2} than T_{H1} (24)	550.825277	-2.851495							
	ENSG00000137265	IRF4	induced by TCR signaling \rightarrow upregulation of inhibitory receptor/impairs metabolism \rightarrow T-cell exhaustion (25); induction dependent on the signal strength of TCR signaling \rightarrow glycolysational expansion/maintenance of effector function (26)	7024.41145	-1.335874							
	ENSG00000189013	KIR2DL4	receptor for HLA-G, activation prevents cytotoxicity, HLA-G increases expression on CD4+ T-cells (27), increased demethylation of promoter and expression in effector vs. memory T-cells (28)	19.941967	3.054789							
	ENSG00000124772	CPN5	expression higher in effector than memory CD4+ T-cells (29)	603.623657	1.930024							
	ENSG00000168229	PTGDR	higher expression in T_{H1} than other T-cells (30)	371.556901	2.575663							
	ENSG00000165025	SYK	switches TCR signaling from naive/memory to effector CD4+ T-cells (31)	131.51078	2.81686							
	ENSG00000170854	RIOK2	represses expression of IL-4 (32)	264.81806	-1.42225							
	ENSG00000169885	OSM	pro-inflammatory cytokine, attracts macrophages, induces antiviral response in epithelial cells (33, 34)	1983.6564	-1.98649							
	ENSG00000162968	SATB1	required for suppressive function of T_{H2} and suppressor of effector differentiation (35)	11007.1072	-1.273391							
	ENSG00000108176	DNAJ21	chaperone, co-factor of Hsp70 (36), which induces cytotoxic CD4+ T-cells (37)	113.63151	-3.00366							
	ENSG00000160116	EMX1	accumulates upon early TCR signaling and hypoxia, accumulation increases glycolysis/G2M, expression diminished upon administration of IL-2, increased upon administration of IL-4, sustained effector function of CD8 CTLs (12)	3957.09145	-1.554453							
	ENSG00000169194	IL13	synergizes with IL-2 in regulating interferon-gamma synthesis (38)	481.784448	-2.918254							
	ENSG00000149295	DRD2	dopamine receptor, drives Tau differentiation via T-bet and IFN γ production, decreases CD25 and CD69, advances T-cell differentiation, helps NFkB activation (22)	30.4424689	-3.125411							
	ENSG00000154465	TNFRSF11A	RNAK1, increases T-cell survival upon binding of RANKL (39); RANKL increases IFN γ secretion T-cells (40)	1997.55281	-2.813605							
	APOPTOSIS	anti-apoptotic										
		ENSG00000118513	MYB	promotes memory T-cell development, antiapoptotic via Bcl-1 (41)	1103.23321	-3.78842						
		ENSG00000141655	TNFRSF11A	RANKL increases T-cell survival upon binding of RANKL (39); RANKL increases IFN γ secretion in effector and memory T-cells (40)	1997.55281	-2.813605						
		ENSG00000134278	SPFR1	involved in DNA repair (42)	205.11297	-2.942319						
		ENSG00000134853	PDGFRA	anti-apoptotic signaling via PI3K/migration (43)	124.06083	-4.193055						
		ENSG00000205755	CHRF2	thyric stromal lymphopoiesis receptor, closely related to gamma chain, expression increased after TCR activation, signaling increases survival of T-cells and proliferation of activated CD4+ T-cells (44)	130.186039	-1.804407						
ENSG00000128778		SIRT1	allows Tau expansion in Rapamycin (10), antipoptotic/upregulated in Tau vs. Tau (11)	95.262504	-3.407825							
ENSG00000102096		PIK2	allows Tau expansion in Rapamycin (10), antipoptotic/upregulated in Tau vs. Tau (11)	794.4009	-1.752741							
ENSG00000138026		IGKAP	p63, can suppress p73-dependent apoptosis (46)	825.271346	-2.023846							
ENSG00000140443		IFR4	increased in autoimmunity, increased upon TCR stimulation, ligand binding enhances proliferation and survival of CD45RO+ T-cells (17)	797.424827	-1.791784							
ENSG00000180534		TPSTY15	decreases p53 levels (47)	98.8277414	-1.991591							
ENSG00000131343		BEX3	protects against mitochondrial apoptosis, positively regulates Bcl-2/NFkB pathway and negatively regulates BAD, BAK1 and PUMA (48)	199.28887	2.151393							
ENSG0000011028		MRC2	Mannose receptor, extends survival of mouse thymocytes/maintains cell growth (49)	208.370967	-3.100144							
ENSG00000171980		C3AR1	activation by C3a enhances naive CD4+ T-cell activation, survival and proliferation via PI3K/Akt (50)	200.019164	-2.171075							
ENSG00000101752		MEI1	E3 ubiquitin ligase, antagonizing anti-apoptotic effects of DAPK1 to promote TNF-induced apoptosis (51)	7311.88339	-1.07792							
ENSG00000163568		AIM2	sensor of cytoplasmic DNA activating inflammasome and cell death (52)	539.820633	-1.805941							
T-CELL ACTIVATION		ENSG00000128322	IGLL1	downregulated within 48 - 96 h after T-cell activation (53)	28.8096993	-3.188403						
		ENSG00000114728	AC10RB2	downregulated upon activation in naive T-cells (54)	893.595947	-1.83528						
		ENSG00000183386	PMOCh	expressed activation dependently in T_{H1} , but not T_{H2} cells (55), upregulated in induced Treg (56)	520.59482	-1.970519						
		ENSG00000139946	PEL12	cooperates with Bcl-10 to activate NFkB in mice; can activate MAPK and AP-1/IEK-1 in humans (57)	2995.12322	-3.12598						
	ENSG00000134480	IL6RA	CD25, sign for terminal differentiation in chronic viral infection (58)	620.12175	-2.47526							
	ENSG00000105946	EBI3	part of IL-27 and IL-35, expressed in CD4/CD8 T-cells upon activation with phytohemagglutinin and IL-27 (59)	-4.278035	7.865508							
	ENSG00000118283	KLIF7	upregulated in activated CD8+ T-cells (60)	-2.279037	1.10E-08							
	ENSG00000147408	CSGALNACT1	associated with EAE (61)	-2.046745	8.2E-07							
	ENSG00000104427	ZGN2A1C	variant increases susceptibility to MS (62)	-2.444141	9.38E-07							
	ENSG00000171980	CSMR1	activation by C3a enhances naive CD4+ T-cell activation, survival and proliferation via PI3K/Akt (50)	2.171075	5.84E-08							
	ENSG00000168811	IL12A	required for development of EAE (63), upregulates IL12R \rightarrow signaling induces T-bet (64)	-2.749978	1.78E-05							
	ENSG00000151748	SAV1	part of Hippo signaling (induces a rather inflammatory T-cell phenotype (65))	-1.437997	2.07E-05							
	ENSG00000214711	CAPN14	calpain, can generate constitutively active calcineurin (66)	-2.500567	3.48E-05							
	ENSG00000174136	RGMB	ligand for PD-L2, not increased upon T-cell activation and absent in naive mice, sets down the threshold for activation and supports T-cell expansion (67)	-2.820545	0.001115							
	ENSG00000127883	TNFRSF19	increases proliferation and NFkB signaling (68)	-2.807645	0.000155							
	ENSG00000111252	SH2B3	LNK, involved in TCR signaling via PI3K/PLC γ /Ras (69)	1.242567	0.000290							
	ENSG00000188822	CMP2	carnitine/inositol receptor 2, inhibits inflammatory cytokines/proliferation of T-cells (70)	264.685093	2.458243							
	ENSG00000133089	TMCC2	upregulated in the absence of IL-6 which is downstream of TCR signaling (71)	130.965562	-1.640783							
	ENSG00000154127	UBASH3B	negatively regulates TCR signaling (72)	880.821715	1.94863							
	ENSG00000107679	PLEKHA11	reduces activation of PI3K/Akt and STATs via PTPN11 (73)	1089.23164	1.942193							
ENSG00000157075	TRB2	negative regulator of mitogen-activated protein kinases, differential expression in peripheral CD4+ (higher) and CD8+ T-cells (74)	2082.21767	1.612003								
TRANSPORTERS / ION CHANNELS / GAP_JUNCTIONS	ENSG00000052098	SLC22A17	iron transporter, down-regulated in Tau compared to Tau (75)	52.2089151	-4.821621							
	ENSG00000173150	PANX2	Structural component of the gap junctions and the hemichannels	38.9683951	-4.153572							
	ENSG00000138052	SLC14A2	Transport of glucose and other sugars, bile salts and organic acids, metal ions and amine compounds, induced by TNF (76)	458.502097	-2.894748							
	ENSG00000069923	SLC9A7	sodium and potassium+ proton antiporter, lower expression in non-human primate EboA survivors than in non-survivors (77)	1991.43457	-1.812689							
	ENSG00000144935	TRPC1	needed for intracellular calcium increase by TH1 in T-cells via DAG (78)	328.047316	-2.158811							
	ENSG00000105674	GJB2	connexin 26, part of gap junctions	38.2806533	-3.677982							
	ENSG00000121742	GLBE	connexin, part of gap junction	44.956475	-3.42867							
	ENSG00000075673	ATP12A	H K^+ -ATPase	231.196155	-3.834569							
	ENSG00000180502	SLC24A3	Potassium-dependent sodium/calcium exchanger	49.8368198	3.227841							
	ENSG00000122986	HVCN1	voltage-gated proton channel activity, downregulated in CD56+ T-cells (able to kill CMV-infected cells), associated with metabolism (79)	469.805016	0.929571							
	ENSG00000135750	KCNK1	contributes to passive transmembrane potassium transport	36.3723901	-2.73024							
	ENSG00000160190	SLC37A1	PI-linked GSP antiporter (80)	8028.32349	1.509443							
	ENSG00000182747	SLC35D3	Solute Carrier	12.9025324	-2.966805							
	ENSG00000091137	SLC26A4	transmembrane transporter	125.84343	-2.113035							
	ENSG00000186187	ZNRF1	regulates the sodium/potassium pump (Na $^+$ /K $^+$ -ATPase) with ZNRF2 (81), high expression in conventional T-cells in the lymph node, but not skin or fat (82)	734.851294	-1.470285							
	ENSG00000165449	SLC16A9	Proton-linked monocarboxylate transmembrane transporter	14.7888121	-2.481201							
	PROLIFERATION	ENSG000000196507	TCEAL3	transcription elongation factor	98.9871397	-2.19082						
		ENSG00000175155	YPEL2	part of the mitotic apparatus required for cell division (83)	1404.32006	-1.19115						
		ENSG00000048886	CH3L2	activation of ERK1/2 phosphorylation by CH3L2 inhibits cell mitogenesis and proliferation (84)	183.237131	1.18076						
		ENSG00000102302	NME4	involved in Pyrimidine Metabolism and Metabolism	325.68844	-1.87288						
ENSG00000174136		RGMB	involved in T cell activation and supports T-cell expansion (67)	181.82579	-2.82547							
ENSG00000127863		TNFRSF19	cell cycle regulated NADPH-dependent dicarboxylate reductase enzyme (85)	52.286621	-2.60785							
ENSG00000106887		DHR22	ligand for UDP-glucose, activation inhibits murine T cell proliferation (86)	68.738987	-2.18412							
ENSG00000174844		P2RY14	ligand for UDP-glucose, activation inhibits murine T cell proliferation (86)	28.1452621	-2.54096							
ENSG00000164362		TERT	Telomerase Reverse Transcriptase, overexpression extends proliferative potential of human T-cells (

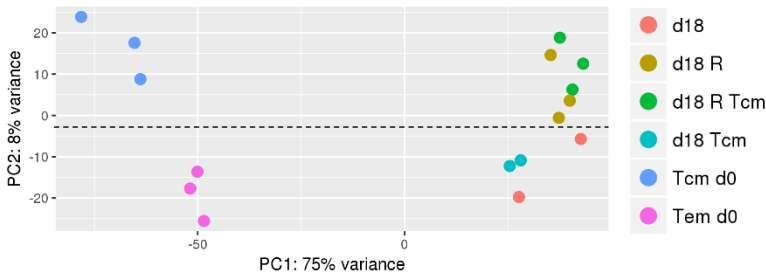


Figure S2: Rapamycin-treated cells are closer to *ex vivo* sorted T_{CM} and non-treated cultures resemble T_{EM} in dimension PC2.

Principle component (PC) analysis of RNA sequencing data of T_{CM} and T_{EM} sorted on d0 out of PBMCs derived from buffy coats of $n = 3$ HDs and untreated as well as Rapa-TCPs (R) and T_{CM} -like cells sorted on d18 of culture from the indicated TCP derived from the same $n = 3$ buffy coat donors. Lacking data points of d18 and d18 T_{CM} occurred due to failure at the quality control level.

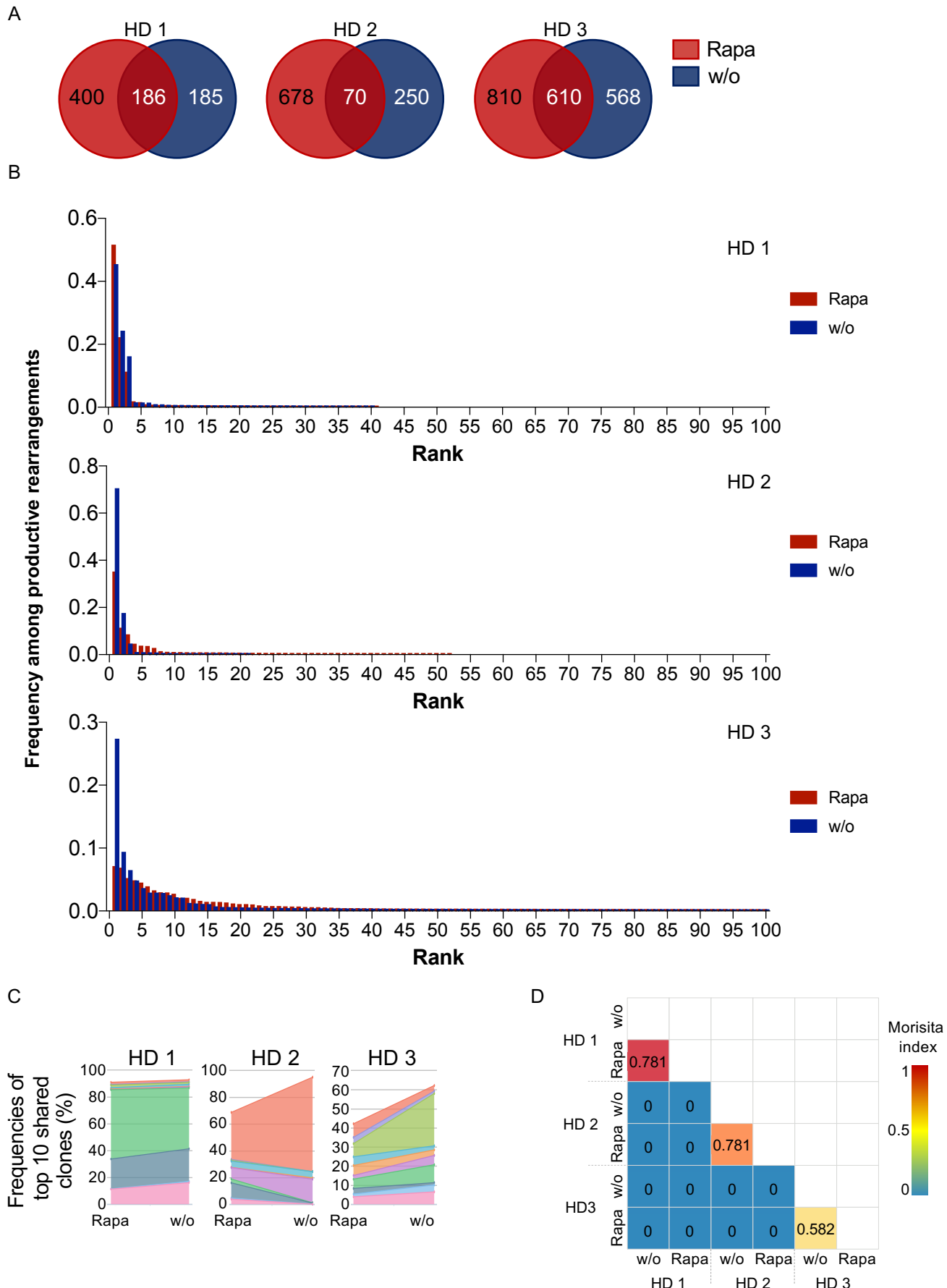


Figure S3: Distribution of T-cell clones among Rapa- and untreated TCPs and different donors.

A: Venn diagrams of all clones of Rapa- (red) and untreated TCPs (blue) of 3 HDs demonstrating individual and shared clones of each sample. **B:** Frequencies among productive rearrangements of the top100 clones of Rapa- (red) and untreated TCPs (blue) of 3 HDs. **C:** Stacked view of individual frequencies of the top 10 most represented shared clones in Rapa- and untreated TCPs (w/o) of 3 HDs. Shared clones were ranked based upon the maximum frequency achieved in either Rapa- or untreated TCPs. **D:** Morisita index matrix showing sample overlap between all samples, which is based on the presence of unique clones, individual frequencies of clones and the probability of a common origin of two samples. All data were calculated in ImmunoSEQ-Analyzer 3.0 based on TCR β sequencing data.

Table S2: Patient details.

Pred. = Prednisolone; M-pred. = Methyl-prednisolone; Tac. = Tacrolimus; MMF = Mycophenolate mofetil; MPS = Mycophenolate sodium; CSA = Cyclosporine A; VGCV = Valganciclovir; ACV = Acyclovir; conc. = concentration; imcomp. = incompatible

No.	Patients with so far no recorded CMV viremia									Patients with recent CMV viremia				Patients with history of CMV viremia					
	1	2	3	4	5	6	7	8	9	10	11	12	13	14	15	16	17	18	19
Age	58	45	42	53	29	45	51	44	78	56	52	46	63	70	66	67	34	60	
Gender	M	F	F	F	M	M	F	M	M	M	M	M	M	M	F	F	F	F	
Time from KTx [d]	264	294	161	19	21	21	13	21	694	27	2399	28	1809	296	380	563	665	7418	
Time from last CMV viremia [d]	-	-	-	-	-	-	-	-	0	0	13	9	1728	119	140	112	645	40	
Tac. blood conc. [ng/ml]	8.5	6.4	7.2	11.3	10	8.35	5.2	9.7	6.5	11.5			5.9	5.5	8.5	11.3	4.1	4	
Immunosuppression at d0	Tac (1 mg) MMF (1.5 g)	M-pred (4 mg) Tac (10.5 mg) MMF (2 g)	Tac (3 mg) MMF (1.5 g)	Pred (20 mg) Tac (15 mg) MMF (2 g)	M-pred (4 mg) Tac (18 mg) MMF (2 g)	M-pred (4 mg) Tac (6 mg) MMF (2 g)	M-pred (24 mg) Tac (8 mg) MMF (2 g)	M-pred (4 mg) Tac (16 mg) MMF (2 g)	M-pred (4 mg) Tac (3 mg) MMF (1.5 g)	M-pred (4 mg) Tac (10 mg) MMF (1.5 g)	M-pred (4 mg) CSA (130 mg) MMF (2 g)	M-pred (4 mg) CSA (250 mg) MPS (2 g)	M-pred (4 mg) Tac (4.5 mg)	M-pred (4 mg) Tac (7 mg) MMF (500 mg)	M-pred (4 mg) Tac (3.5 mg) MMF (1.5 g)	M-pred (4 mg) Tac (2.5 mg) MMF (2 g)	M-pred (4 mg) Tac (7 mg)	Pred (5 mg) Tac (4.5 mg) MPS (108 g)	
Rejection [from d0]	scale cellular rejection (<245)	no	no	no	no	suspected scale (ATG-17 to -19)	no	no											
Antiviral therapy [from d0]	none	none	none	none	none	none	none	none	VGCV 900 mg (488 to 420); 450 mg (-283 to -356); 225 mg (-488 to -596); +356 to -374)	VGCV 450 mg (19.01.2017 - 14.02.2017); 900 mg (23.11.2016 - 19.01.2017)	VGCV 450 mg (2451 to 2423)	VGCV 900 mg (7 to +5)	none	VGCV 450 mg (-1267 to -1218); -1372 to -1311)	VGCV 225 mg (-355 to -327)	none	none	ACV 200 mg (since -753)	
Other detected CMV/viremia [from d0]	none	none	none	none	none	+54	none	+112; +7	+400; -283; +261; +168; +119; +78; +45; -35; +6; -125; -292; -312; -348; -391; -412; -420; -475; -491; -486	+266; -7; -11; -14; 21	+488; +272; +97; -13; -22; -78; -287; -637; -813; -978; -1182; -1569; -2470; -2489	-18; -25	none	+325; +252; -524; -708; -888; -1255; -1269	+328; -233	487; -528; -538	none	+297; +129; -207; -613; -641; -972; -2324	
Lymphocyte count [1/dl]	1.04	1.49	1.48	2.34	1.23	0.09	2.34	2.32	0.28	0.47	0.71	1.21	1.6	0.98	0.88	1.22	1.26	-	
Donor CMV before KTx	CMV-; living	CMV+; living	CMV-; living	CMV+; living	CMV+; living	CMV-; living	CMV+; living	CMV+; living	CMV+; decreased	CMV+; living	CMV+; living	CMV+; living	CMV+; decreased	CMV+; decreased	CMV+; decreased	CMV+; decreased	CMV+; living	CMV+; decreased	
Other						ABO incomp. donation, delayed graft function												missed abortion (-1)	renal carcinoma (diagnosed +289)
Underlying disease	IgA nephritis	hypertensive nephropathy	polycystic kidney disease	IgA nephritis	IgA nephritis	seronegative Lupus erythematosus	polycystic kidney disease	left nephrectomy after relapsed pyelonephritis obstructive nephropathy	hyperertensive nephropathy	IgA nephritis	unilateral renal agenesis and obstructive nephropathy	Renal hypertensive angiopathy	Pauci-immun glomerulonephritis	unclear	Diabetic nephropathy	hypertensive nephropathy	IgA nephropathy	Diabetic nephropathy	

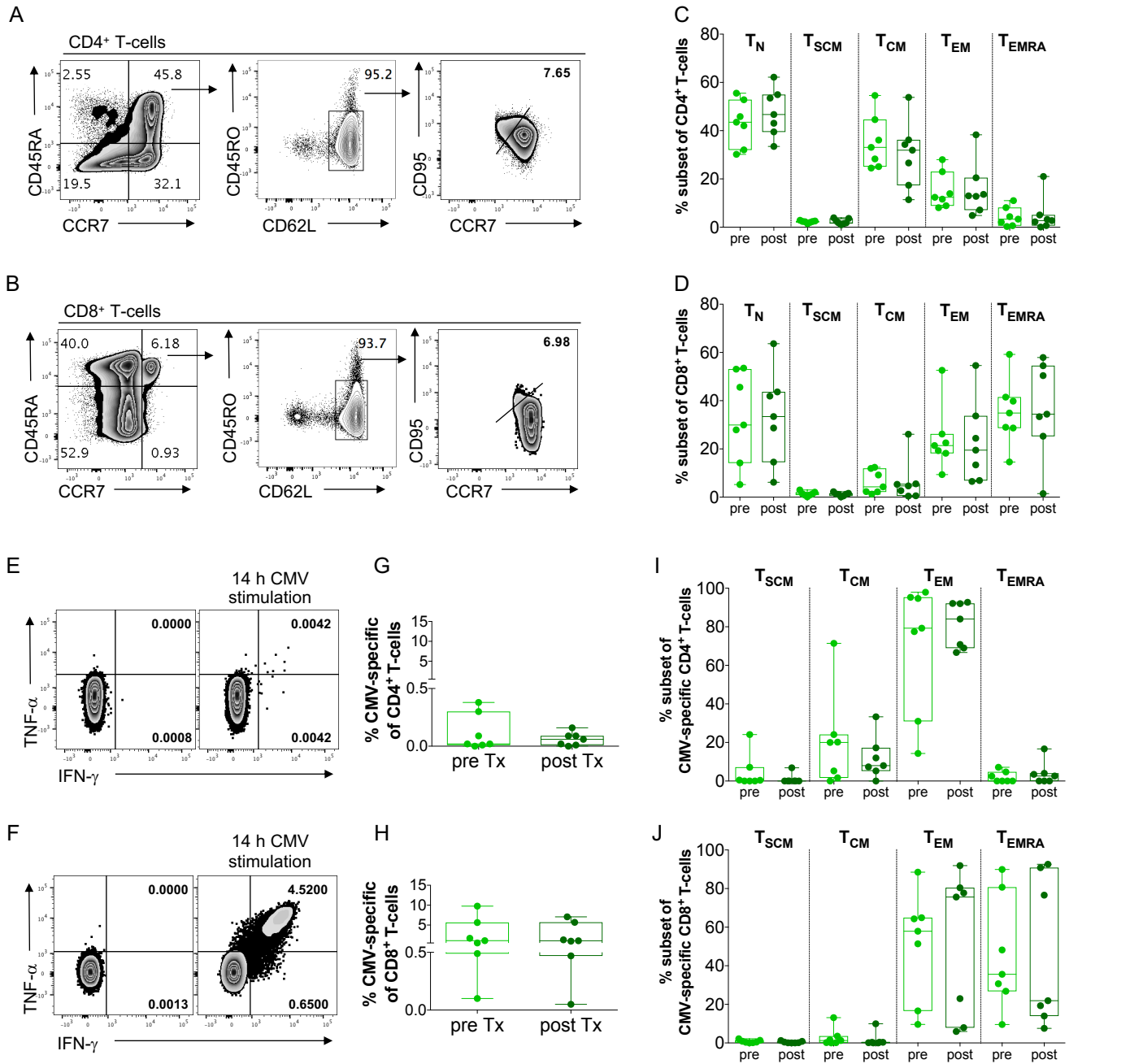


Figure S4: CMV-specific *ex vivo* response shifts to T_{EM} on the expense of T_{CM} within a few weeks after transplantation while the global subset composition remains stable.

N = 7 paired samples from the same patients before (pre; pastel green) and a few weeks after KTx (post; dark green). Gated on lymphocytes (FSC-A vs. SSC-A), single cells (FSC-H vs. FSC-A), living T-cells (CD3 vs. life/dead-discriminating dye) and as indicated on CD4⁺ or CD8⁺ T-cells, respectively. Gating strategy for discrimination of T-cell memory subsets for CD4⁺ (A) and CD8⁺ (B) subsets: T_N: CD45RA⁺ CCR7⁺ CD95⁻; T_{SCM}: CD45RA⁺ CCR7⁺ CD45RO⁻ CD62L⁺ CD95⁺; T_{CM}: CD45RA⁻ CCR7⁺; T_{EM}: CD45RA⁻ CCR7⁻; T_{EMRA}: CD45RA⁺ CCR7⁻. Global T-cell memory subset distribution of CD4⁺ (C) and CD8⁺ (D) T-cells from peripheral blood collected *pre-* and *post-Tx*. Subsets gated as shown in A/B. IFN γ and TNF α were stained intracellularly after 14 h stimulation of fresh PBMCs with CMV_{E-1/pp65} peptide pools and addition of BFA after 1 h. Exemplary dot plots and gating strategy for CD4⁺ (E) and CD8⁺ (F) T-cells. Summary of CMV-specific CD4⁺ (G) and CD8⁺ (H) T-cells identified as IFN γ ⁺TNF α ⁺ detected *ex vivo* in PBMCs of KTx patients based on the gating strategy shown in E/F. Proportions of subsets among CMV-responsive CD4⁺ (I) and CD8⁺ T-cells (J) determined by characteristic expression of CCR7, CD45RA and CD95. Gates were applied from gates set for global T-cell subset distribution (A/B).

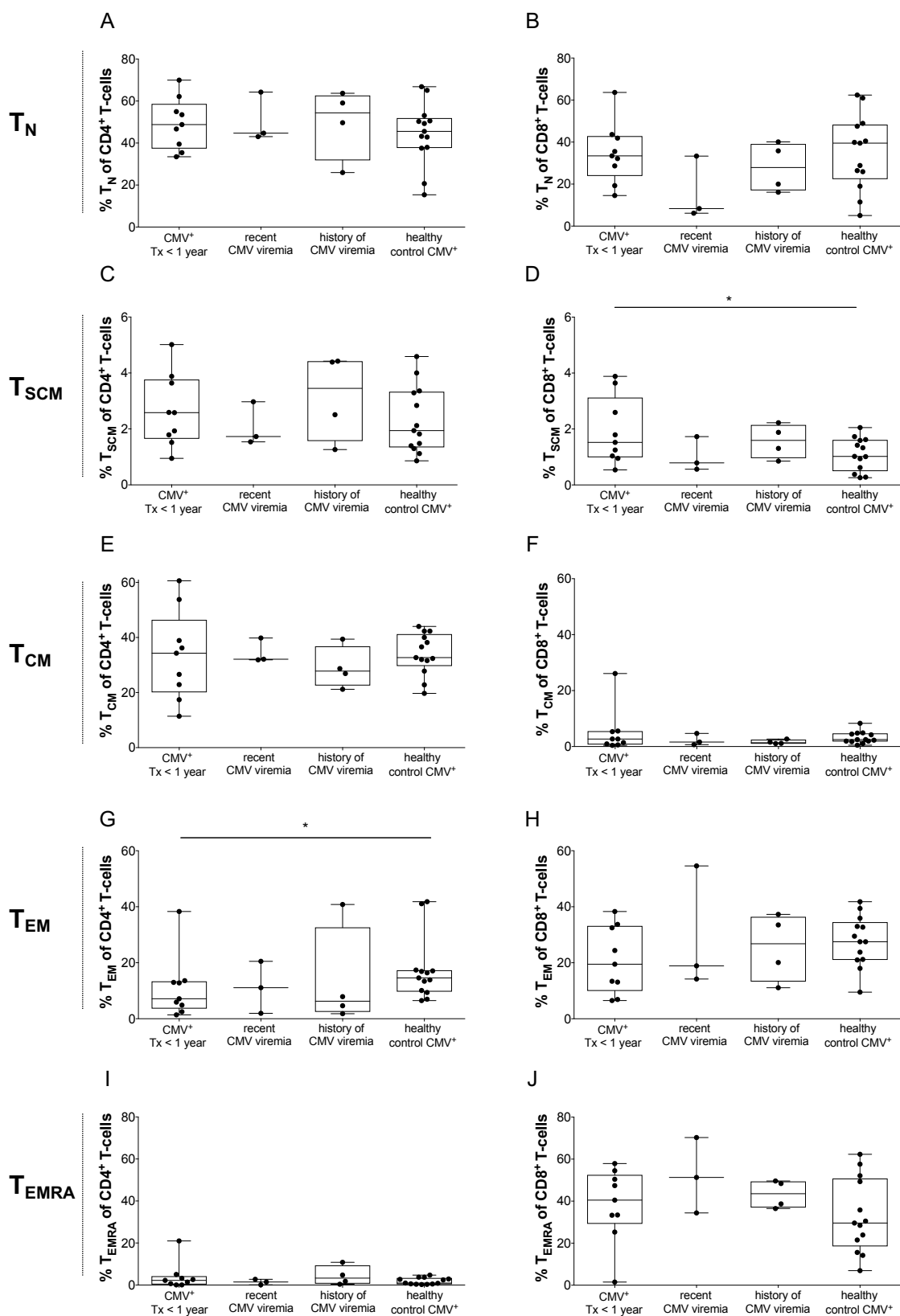


Figure S5: $CD8^+ T_{SCM}$ are globally increased and $CD4^+ T_{EM}$ globally decreased in the blood of patients without record of CMV viremia compared to the blood of healthy donors.

T-cell subset distribution of $n = 19$ patients (9 with so far no recorded CMV viremia and 6 with a history of CMV viremia)/13 HDs. Global proportions of different $CD4^+$ (left panel) and $CD8^+$ T-cell (right panel) subsets determined by characteristic expression of CCR7, CD45RA, CD62L, CD45RO and CD95. $N=19$ patients (9 with so far no recorded CMV viremia; 4 with recent CMV viremia and 6 with a history of CMV viremia)/13 HDs. Gating strategy is shown in Fig. S4A/B. $CD4^+$ (A) and $CD8^+$ (B) $CD45RA^+ CCR7^+ CD95^- T_N$. $CD4^+$ (C) and $CD8^+$ (D) $CD45RA^+ CCR7^+ CD62L^+ CD45RO^- CD95^+ T_{SCM}$. $CD4^+$ (E) and $CD8^+$ (F) $CD45RA^- CCR7^+ T_{CM}$. $CD4^+$ (G) and $CD8^+$ (H) $CD45RA^- CCR7^- T_{EM}$. $CD4^+$ (I) and $CD8^+$ (J) $CD45RA^+ CCR7^- T_{EMRA}$. All data tested for normal distribution of data points with Kolmogorov-Smirnov test; significance determined with paired t test if normally distributed or Wilcoxon's matched-pairs signed rank test for not normally distributed samples. P-values below 0.05 are indicated by * and defined to be significant.

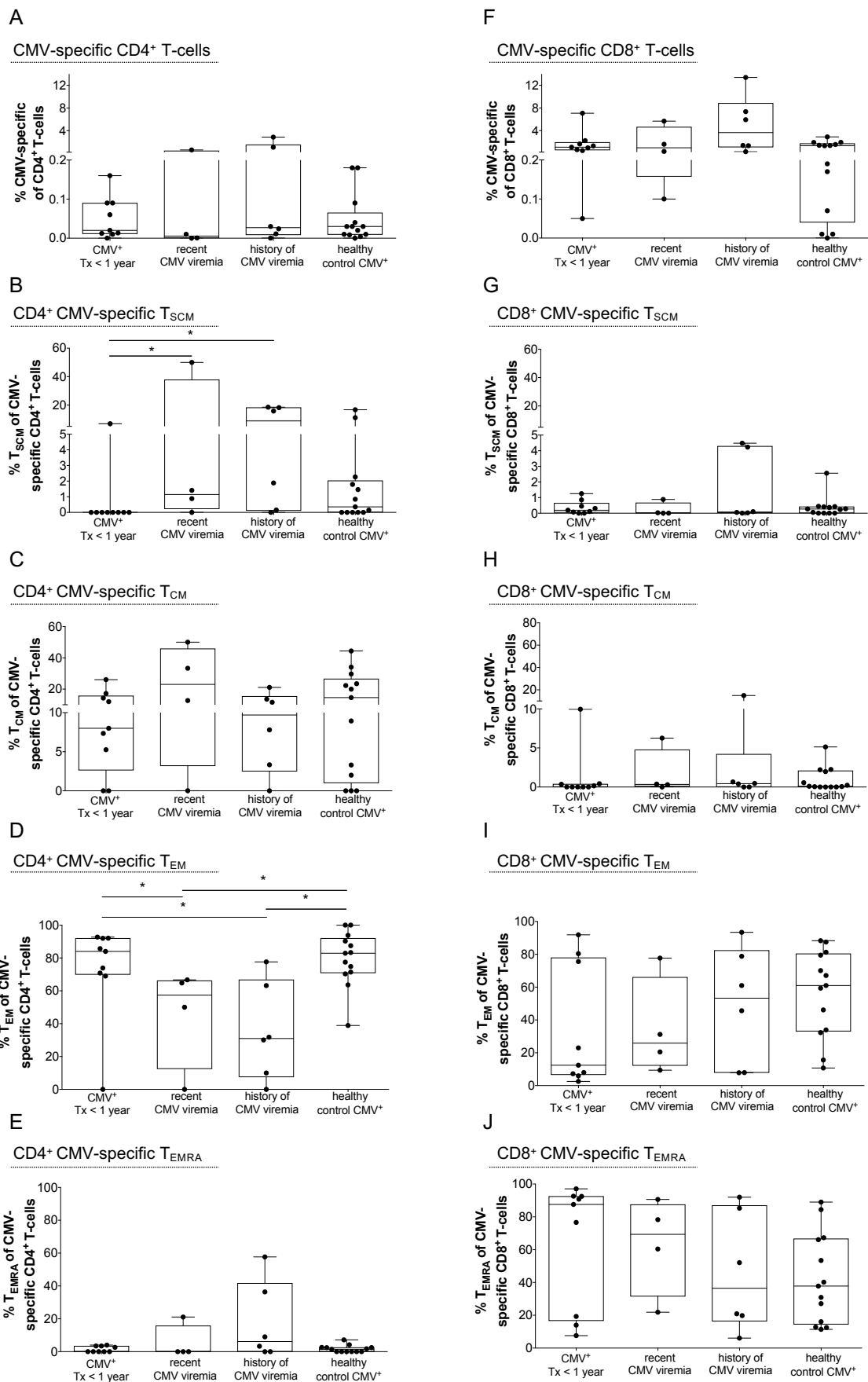


Figure S6: CD4⁺ CMV-specific T_{SCM} accumulate upon CMV reactivation and T_{EM} diminish after a history of CMV viremia in renal transplant recipients.

N=19 patients (9 with so far no recorded CMV viremia; 4 with recent CMV viremia and 6 with a history of CMV viremia)/13 healthy controls. Proportions of CMV-responsive among CD4⁺ (A) and CD8⁺ (F) T-cells detected by double positive intracellular staining for IFN γ and TNF α after 14 h stimulation of fresh PBMCs with CMV_{IE-1/pp65} peptide pools and addition of BFA after 1 h (see dot plots Fig. 4E-F). T-cell memory subset distribution of CMV-reactive CD4⁺ (B-E) and CD8⁺ (G-J) T-cells following the gating strategy and subset definitions presented in Fig. S4A/B, applying gates for global subset distribution from Fig.S4. CMV-reactive CD4⁺ (B) and CD8⁺ (G) CD45RA⁺ CCR7⁺ CD62L⁺ CD45RO⁻ CD95⁺ T_{SCM}. CMV-reactive CD4⁺ (C) and CD8⁺ (H) CD45RA⁻ CCR7⁺ T_{CM}. CMV-reactive CD4⁺ (D) and CD8⁺ (I) CD45RA⁻ CCR7⁻ T_{EM}. CMV-reactive CD4⁺ (E) and CD8⁺ (J) CD45RA⁺ CCR7⁻ T_{EMRA}. All data tested for normal distribution of data points with Kolmogorov-Smirnov test; significance determined with paired t test if normally distributed or Wilcoxon's matched-pairs signed rank test for not normally distributed samples. P-values below 0.05 are indicated by * and defined to be significant.

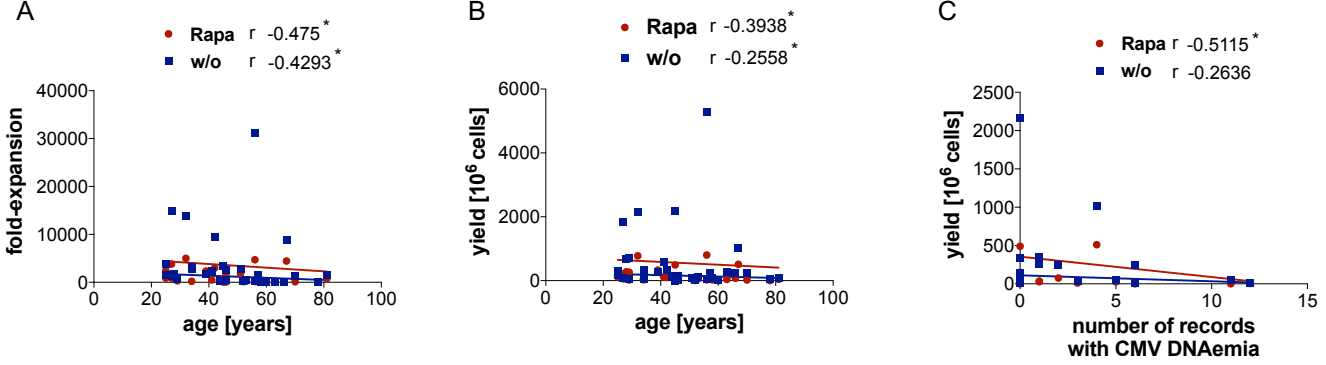


Figure S7: Decreased fold-expansion and yield correlate with increasing age and numbers of recorded reactivations.

Correlations of age and fold-expansion (**A**)/yield (**B**) as well as records of reactivations determined by viremia and yield (**C**) in untreated (blue) and Rapa (treated with 20 nM Rapamycin; red)-TCPs of 19 patients and 13 HDs; distributions tested for normality with Kolmogorov-Smirnov test, correlations of normally distributed data calculated with Pearson's correlation coefficient and of not normally distributed data with Spearman's rank correlation.

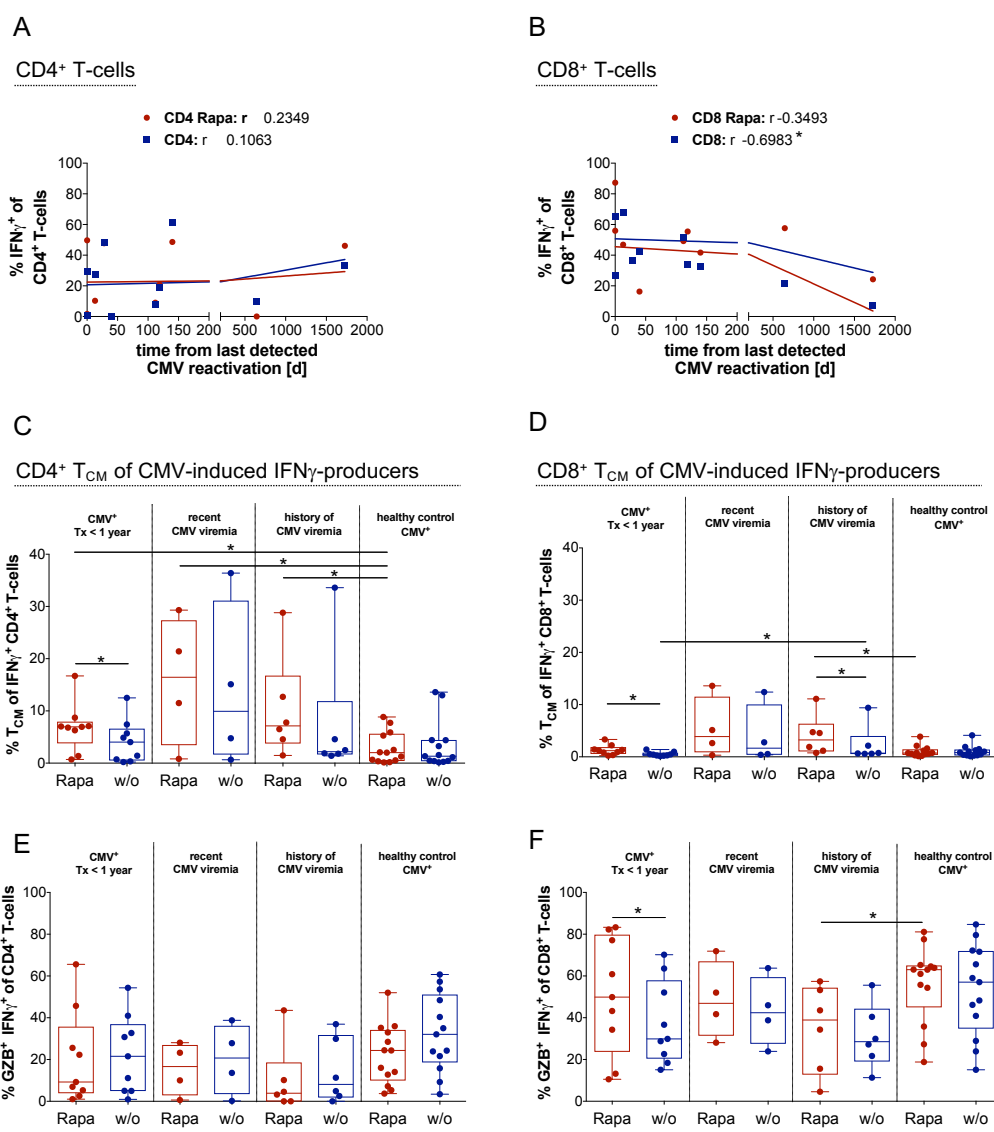
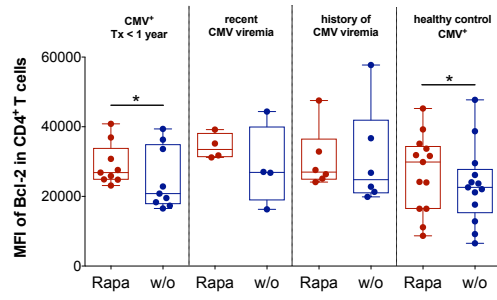
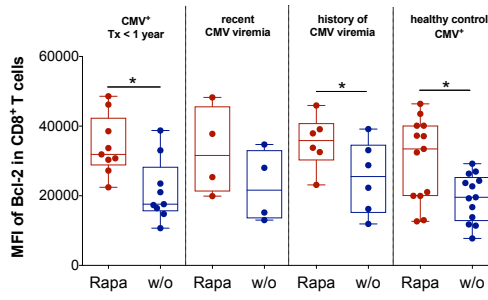
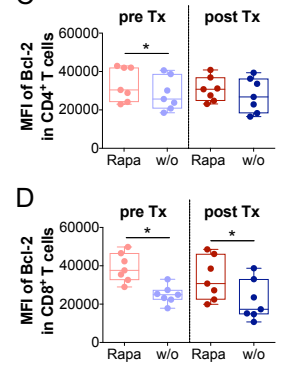
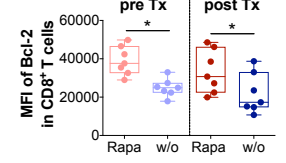


Figure S8: The proportion of IFN_γ-producing CD8⁺ T-cells negatively correlates with the time from reactivation in *Rapa*-TCPs, among CMV-stimulated IFN_γ responders the frequency of T_{CM} is increased in TCPs from patients with recorded CMV viremia and a substantial amount of cytotoxic CD4⁺ T-cells is abundant in TCPs.

Correlations of proportions of IFN_γ-producing CD4⁺ (A) and CD8⁺ (B) T-cells from untreated (w/o, blue) and *Rapa* (red)-TCPs to time from last recorded CMV DNAemia from n = 10 patients (for whom a record of CMV DNAemia was available; Table S2); distributions tested for normality with Kolmogorov-Smirnov test, correlations of normally distributed data calculated with Pearson's correlation coefficient and of not normally distributed data with Spearman's rank correlation. Proportions of CD45RA-CCR7⁺ T_{CM} among IFN_γ producing CD4⁺ (C) and CD8⁺ (D) T-cells. Gates were applied from gates set for global T cell subset distribution (Fig.S4A-B). Proportions of CD4⁺ (E) and CD8⁺ (F) GZB-IFN_γ-double-producers detected by intracellular staining after 6 h stimulation with autologous LCLs loaded CMV_{IE-1/pp65} peptide pools and addition of BFA after 1 h on d21.

A**CD4⁺ T-cells****B****CD8⁺ T-cells****C****D****Figure S9: Bcl-2 is increased also in patient TCPs, especially in CD8⁺ T-cells.**

MFI of Bcl-2 in CD4⁺ (A) and CD8⁺ (B) T-cells of untreated (w/o, blue) and Rapa (red)-TCPs of n = 19 patients (9 with so far no recorded CMV viremia; 4 with recent CMV viremia and 6 with a history of CMV viremia)/13 healthy controls. MFI of Bcl-2 in CD4⁺ (C) and CD8⁺ (D) T-cells of untreated (w/o, blue) and Rapa (red)-TCPs of n = 7 patients for which TCPs were generated before and a few weeks after KTx.